DOI: 10.1002/adsc.200700196

Integrating Catalyst and Co-Catalyst Design in Olefin Polymerization Catalysis: Transferable Dianionic Ligands for the Activation of Late Transition Metal Polymerization Catalysts

Mikaël Brasse,[a] Juan Cámpora,[a,*] Maxwell Davies,[a] Emmanuelle Teuma,[a] Pilar Palma,[a] Eleuterio Álvarez,[a] E. Sanz,[a] and Manuel L. Reyes[b]

[a] Instituto de Investigaciones Químicas, Consejo Superior de Investigaciones Científicas-Universidad de Sevilla, c/Américo Vespucio 49, 41092 Sevilla, Spain
Fax: (+34)-954-460-565; e-mail: campora@iiq.csic.es
[b] Centro de tecnología Repsol-YPF, Carretera de Extremadura NV, Km 18, 28930 Móstoles, Madrid, Spain

Received: April 18, 2007; Published online: September 11, 2007

Supporting information for this article is available on the WWW under http://asc.wiley-vch.de/home/.

Abstract: Treatment of nickel and palladium α-diimine catecholate complexes with alkylaluminum catecholates leads to active ethylene polymerization catalysts. Comparison of the catalytic activities achieved with combinations of α-diimine catecholate or halide complexes as catalyst precursors with different activators (MMAO or alkylaluminum catecholates) reveals that the presence of the catecholate ligand in both catalyst components is beneficial for achieving high activity levels at very low M/Al ratios.

Keywords: aluminum; catalyst design; nickel; palladium; polymerization

Introduction

Technical processes for olefin polymerization require the use of suitable co-catalysts to transform inactive but readily prepared and handled catalyst precursors into the active species. Heterogeneous Ziegler–Natta catalysts can be prepared using inexpensive aluminum alkyls, but the successful application of homogeneous catalysts in industrial polyolefin production processes became possible only after the discovery of polymethylalumoxane (MAO) by Kaminsky and Sinn in the early 1980s.[1] The efficacy of MAO or its derivatives as co-catalysts is generally unmatched by other organoaluminum reagents. The ability of these substances to activate many kinds of catalytic precursors has been demonstrated for a wide range of transition metal catalyst precursors, from group 4 metallocenes to group 10 classic coordination complexes.[2,3] However, the practical use of alumoxanes also poses some important drawbacks. For example, they are relatively expensive reagents that, as a general rule, have to be used in large excess to achieve their optimum of efficiency. In addition, since alumoxanes are oligomeric, ill-defined species, their properties may find significant variations depending on the synthesis method or the commercial supplier.[4] Finally, as MAO and their derivatives display limited thermal stability in solution and are pyrophoric materials in the solid state, they are difficult to handle and store, especially when large amounts are required. Therefore, there are important reasons for finding suitable alternatives to replace MAO in olefin polymerization reactions. The quest for new, MAO-free homogeneous polymerization catalysts has led to many important advances, facilitating the progress of mechanistic investigation and revealing the important role of the counter-anion in the polymerization process.[4–6] However, most of these systems rely in the use of sensitive transition metal alkyl complexes and sophisticated boron-based Lewis or protic acids, that are unattractive for practical applications. In this contribution we propose a strategy for the activation of simple and easily handled precursors, based on the complementary design of both the pre-catalyst and the co-catalyst components, devised to favor an efficient generation of active polymerization catalysts. Our approach relies on the exchange of a bidentate, dianionic ligand, initially bound to the transition metal center for a monovalent alkyl group originating in the organoaluminum reagent. As shown in Scheme 1, this exchange process should directly afford an ion pair displaying the characteristic features of a typical olefin polymerization catalyst. In order to favor this process, a highly favorable enthalpic balance of the exchange reaction has to overcome

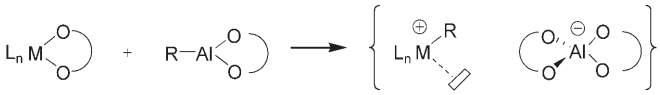

Scheme 1. Formation of the ionic pair by cooperation of the precatalyst and the cocatalyst.

the unfavorable entropic factor posed by the displacement of the chelate from the transition metal center. By choosing late transition metal catalysts, and using an oxygen-based transferable bidentate ligand, we take advantage of the high reactivity of late transition metal-oxygen bonds, originated in their highly polar character[7] and, on the other hand, the oxophilicity and the well known affinity of aluminum complexes for chelating oxygen ligands.[8] Hence, we selected for this study the well-known Ni(II) and Pd(II) α-diimine catalyst systems, using a catecholate-type ligand as a transferable unit. For the co-catalyst component, we also selected catecholate-based organoaluminum reagents. It is expected that the catecholate/alkyl exchange would transform the latter into catecholaluminate anions displaying low affinity for the relatively soft cationic alkylnickel or -palladium species. Perfluorinated aryloxometallate anions based on group 3, 5 and 13 elements have been successfully employed as counteranions in olefin polymerization reactions before.[9] One of the problems found with these cocatalysts is deactivation by transfer of an aryl oxide unit to the cationic center, which could be minimized by the use of chelating catecholates. For the present work, we have selected the derivatives of the commercially available 2,3,4,5-tetrachlorocatechol rather than its perfluorinated analogue. The significantly larger size of the chlorine atoms may have some advantage, contributing to shield the oxygen atoms of the anion, thus decreasing its coordination capability.

Results and Discussion

Synthesis of Ni and Pd α-Diimine Tetrachlorocatecholate Complexes

These complexes were synthesized from the known nickel (**1a, b**) and palladium (**2a, b**) dihalide precursors through straightforward ligand exchange reactions, using potassium tetrachlorocatecholate. The latter is conveniently generated *in situ* by deprotonation of 2,3,4,5-tetrachlorocatecol with potassium *tert*-butoxide in THF (Scheme 2). The four compounds are readily isolated as powdery solids, and X-ray quality crystals of **1′a**, **1′b** and **2′b** have been grown from CH_2Cl_2-hexane solutions by slow solvent evaporation. Although palladium complexes are usually paler than the analogous Ni derivatives, the four compounds display a similar dark blue color, due to a broad absorption band in the low frequency region of their visible electronic spectra.

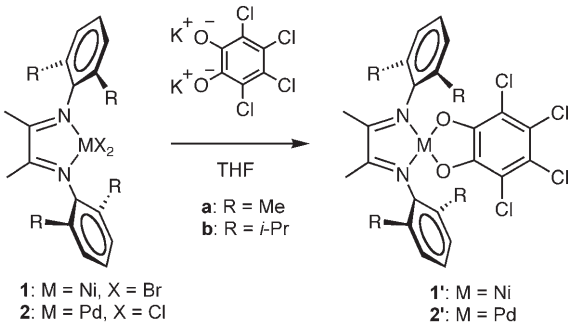

Scheme 2. Synthesis of Ni and Pd α-diimine tetrachlorocatecholate complexes **1′a**, **1′b**, **2′a** and **2′b**.

In contrast with their dihalide precursors (**1**), the nickel tetrachlorocatecholate derivatives **1′** are diamaganetic, and this allows the recording of the NMR spectra of the whole set of complexes. Their ^{1}H NMR spectra are simple and consistent with the highly symmetric structures proposed in Scheme 2, but scarcely informative. The ^{13}C NMR signals of the catecholate ligand are difficult to observe, as they lack any NOE enhancement and are broadened by the quadrupolar moment of the chlorine atoms, but they have been detected for the four complexes. For all of the four complexes, three catecholate resonances are observed: one at low field ($\delta = 158$–159 ppm), due to the oxygen-bound C atoms and two at *ca.* 115 and 117 ppm for the chlorine-bound atoms. These signals appear almost at the same positions in the spectra of the different complexes, suggesting that their electronic structures are little affected by the nature of the metal atom. This is confirmed by the UV spectra which, as already mentioned, are also very similar. The low frequency, color-determining band is likely to originate by a charge transfer transition with a predominantly ligand to ligand character (LL′CT),[10] since its frequency is nearly independent of the metal center, *ca.* 660 nm for **1′a** and **2′a** and 690 nm for **1′b** and **2′b**.

The crystal structures of the two nickel complexes (**1′a** and **1′b**), and the palladium derivative **2′b** are shown in Figure 1, Figure 2 and Figure 3, respectively, and tables of selected bond lengths and angles of these compounds can be found in the Supporting Information. As expected for diamagnetic Ni(II) and Pd(II) complexes, the three molecules display square planar coordination environments, with a slight tetrahedral distortion. The dihedral angles defined by the O−M−O and N−M−N units amount to 6.5° and 4.5°, respectively, in the nickel complexes **1′a** and **1′b**, and is even smaller for the Pd complex **2′b** (3.2°). As mentioned before, the planar configuration of the nickel complexes is somewhat surprising, as Ni(II) diimine complexes with weak-field ligands such as halide are

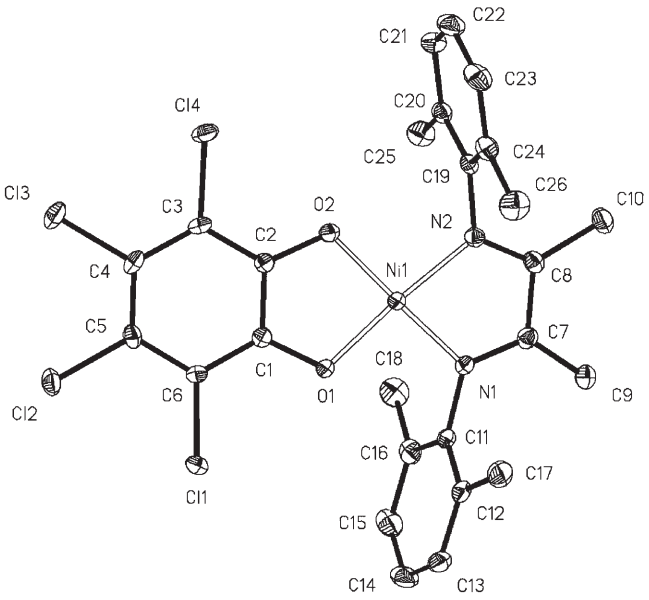

Figure 1. ORTEP view of compound **1′a**.

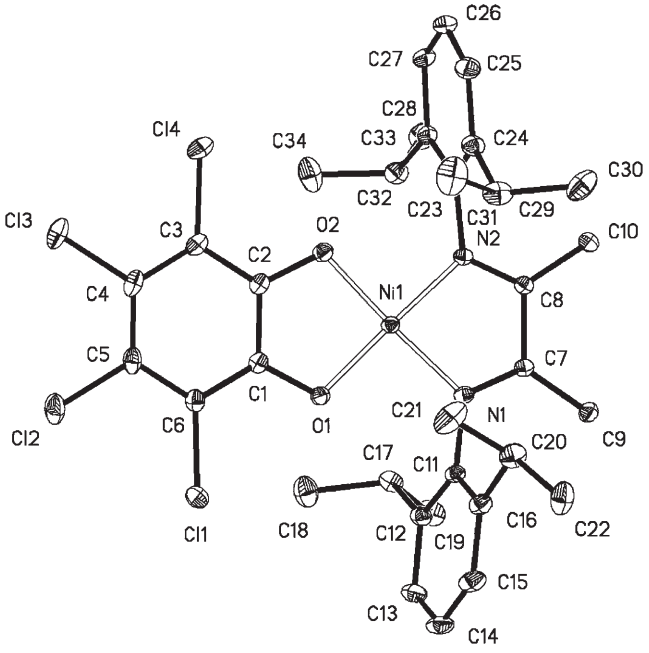

Figure 2. ORTEP view of compound **1′b**.

invariably high-spin, displaying tetrahedral or pentacoordinated structures. Catecholates are usually considered weak field ligands,[11] and the comparison of the averaged M–N bond length in **2′b** (1.984 Å) with those in related square planar complexes PdL_2(α-diimine) displaying the same *N,N′*-bis-(2,6-diisopropylphenyl)diimine ligand appear to confirm this notion. Thus, the dicationic complex with L = MeCN[12] exhibits an almost identical average M–N distance (1.985 Å), while this is shorter in neutral compounds

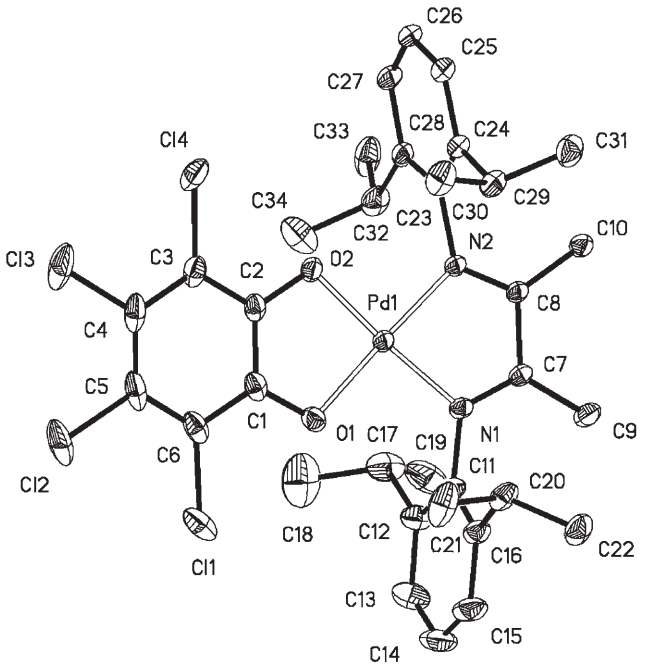

Figure 3. ORTEP view of compound **2′b.**

with L = chloride (2.013 Å)[13] and methyl (2.139 Å).[14] Assuming that the field strength of σ-ligands is directly related to their donor capability (and hence their *trans* influence), this trend indicates that the donor strength of tetrachlorocatecholate is very low, comparable to that of acetonitrile. Therefore, the preference of the nickel derivatives for a square-planar, low spin configuration is probably related to the stability gained by extensive π electron delocalization achieved in such a coordination environment. Catecholate and catecholate-related ligands have received much attention due to their electronically non-innocent character.[15] It is intriguing to consider that the α-diimine and the catecholate groups could actually also behave as a π-electron donor/acceptor system, leading to the bonding situations described in Figure 4.[16] Formal donation of 1 electron from the catecholate to the diimine fragment would lead to the semiquinone(−1) form B, while 2 e^- transfer would result in the formation of a quinone complex and a full reversal of the neutral/anionic donor character of the two chelating ligands. The semiquinone B appears to be favored in the neutral complexes $M(cat)_2$ (M =

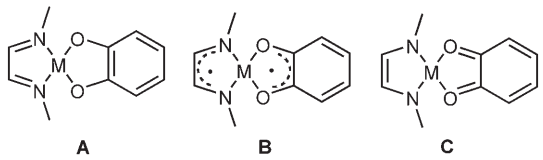

Figure 4. Possible valence-bond isomers describing the structures of α-diimine-catecholate complexes.

Ni, Pd, Pt),[17] a closely related class of compounds where the same valence isomerism situation can also exist. Obviously, the existence of the complexes in the electronic states B or C would be detrimental for our proposal of using catecholate as a transferable dianionic fragment. The length of the C–O and OC–CO bonds can be used as a diagnostic tools to assign the oxidation state of the benzenoid ligand.[15f] Thus, the C–O bond distance in **1′a**, **1′b** and **2′b** (1.32–1.35 Å), compares well with the distance of *ca.* 1.35 Å found in catecholates[17a,b,18] while it is expected to decrease to 1.29 and 1.23 Å in semiquinone[17b,19] and quinone complexes,[17c] respectively, as the bond order increases. However, the OC–CO bond length (*ca.* 1.41 Å in the three compounds), lies in between the figure accepted for catecholates (1.32 Å) and semiquinones (1.44 Å), being 1.53 Å, the value accepted for quinones.[15f] A more rigorous tool to assign the oxidation state of the ligand is the geometrical function Δ, defined as a statistically weighed comparison of the two C–O and six C–C bonds of the benzenoid ligand with those in free catechol and benzoquinone.[20] This parameter takes the value $\Delta = -2$ for catecholate complexes, increasing to −1 in semiquinonates and 0 in pure quinone compounds. For **1′a** and **1′b**, it amounts to −1.9(2), and to −1.8(1) for **2′b**. In addition, the C–C and C=N bonds within the nitrogen ligand fragment of the latter compounds are typical for α-diimine complexes.[12–14] Thus, it can be safely concluded that the structure of these catecholate complexes is appropriately described by the conventional catecholate(−2) representation (**A**) given in Figure 4.

Alkylaluminum Catecholate Complexes

The reaction of catechol with aluminum alkyls "AlR_3" in 2:3 molar ratio has been reported to provide trinuclear complexes of composition $Al_3R_5(cat)_2$.[21] Many other trinuclear complexes displaying the same trinuclear framework have been prepared by reacting different types of diols with aluminum alkyls.[22] In order to obtain formally tricoordinated complexes of composition $[Al(R)(tetrachlororcatecholate)]_n$, we have investigated the reaction of 2,3,4,5-tetrachlorocatechol with trimethylaluminum (TMA) and triethylaluminum (TEA) in non-coordinating solvents (CH_2Cl_2, hexane, toluene), using 1:1 molar ratios. However, these reactions failed to afford the desired compounds, and instead led to the corresponding trinuclear products **3** and **4**, together with large amounts of intractable organoaluminum species. As expected, **3** and **4** are obtained selectively when the reagents molar ratio is adjusted to the stoichiometric 2:3 value (Scheme 3). The two compounds are readily isolated as colorless, non-pyrophoric solids. Their NMR spectra are sharp and display three sets of signals for the

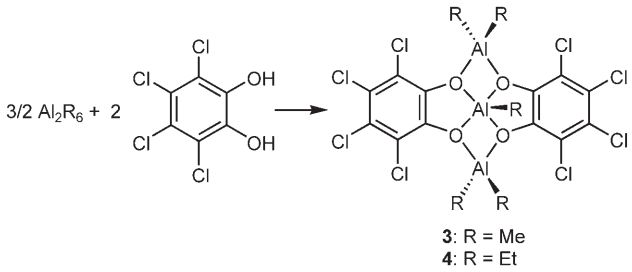

Scheme 3.

R groups with relative intensities 2:2:1, corresponding to the terminal equatorial, terminal axial and to the central aluminum-bonded alkyl groups, respectively.

The crystal structure of compound **3** is shown in Figure 5, and a list of selected bond distances and angles is provided in the Supporting Information. The

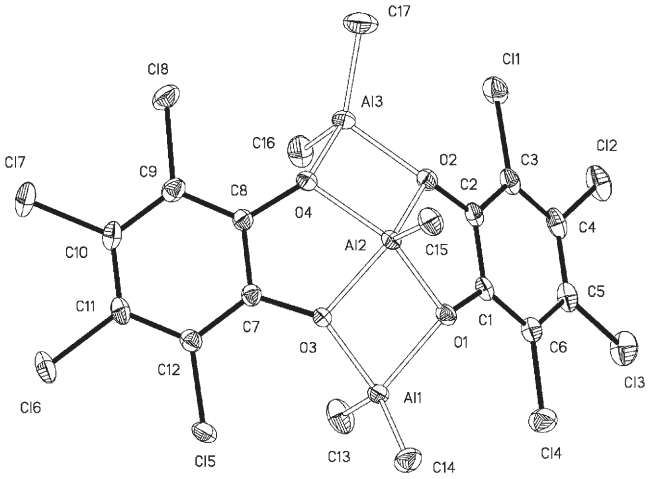

Figure 5. ORTEP view of compound **3**.

molecule contains a central $AlMe(C_6Cl_4O_2)_2$ unit, with two $AlMe_2$ fragments bound to thee oxygen atoms. The central aluminum atom Al-2 exhibits square pyramidal geometry, while the terminal Al-1 and Al-2 are approximately tetrahedral. Overall, the molecule displays a bowl shape, with the pentacoordinated Al-2 placed in the bottom of the cavity. The Al-2···Al-1 and Al-2···Al-3 distances are almost identical (2.947 Å) and are large enough to rule out any metal-metal interaction. The molecule departs from the ideal C_{2v} symmetry due to small albeit significant differences in the Al-2–O bonds, two of them (Al-2–O-1, Al-2–O-4) being *ca.* 0.02 Å longer than the other two (Al-2–O-2, Al-2–O-3). Furthermore, the Al-2–O-1 [1.9220(10) Å] and Al-2–O-4 (1.9199(10) Å] bonds are in fact significantly longer than the average Al(central)–O bond for this kind of compounds (1.879 Å),[23] suggesting that the donor capability of the bridging oxygen atoms may be

Table 1. Ethylene polymerization experiments.[a]

Entry	Catalyst	Cocatalyst	Time [m]	PE Yield [g]	Activity[b]	$T_{1/2}$[c]	M_n[d]	M_w[d]	M_n/M_w	Branch Num[e]
1	**1a**	**3** (3 equivs.)	20	–	13[f]	-	6.37	30.70	4.8	14
2	**1a**	**3** (10 equivs.)	20	–	60[f]	-	5.82	23.03	3.9	12
3	**1a**	MMAO (30 equivs.)	20	0.00	0	-	-	-	-	-
4	**1a**	MMAO (1000 equivs.)	20	3.40	2550	3.7	2.25	7.81	3.5	47
5	**1a**	**3** (1 equiv)	50	0.77	231	-	5.85	33.40	5.7	9
6	**1a**	**3** (2 equivs.)	25	1.30	780	-	4.24	21.40	5.0	17
7	**1′a**	**3** (3 equivs.)	20	1.80	1350	6.6	4.74	23.77	5.0	22
8	**1′a**	**3** (10 equivs.)	20	3.19	2392	6.8	3.18	9.75	3.1	59
9	**1′a**	**4** (3 equivs.)	20	0.60	450	2.3	7.05	28.00	4.0	7
10	**1′a**	**4** (10 equivs.)	25	0.80	480	3.2	3.54	19.48	5.5	15
11	**1′a**	MMAO (30 equivs.)	20	0.00	0	-	-	-	-	-
12	**1′a**	MMAO (1000 equivs.)	20	3.60	2700	5.7	2.15	6.71	3.1	45
13	**1b**	**3** (3 equivs.)	25	0.00	0	-	-	-	-	-
14	**1b**	**3** (10 equivs.)	25	0.00	0	-	-	-	-	-
15	**1b**	MMAO (30 equivs.)	25	0.00	0	-	-	-	-	-
16	**1b**	MMAO (1000 equivs.)	25	2.60	1560	11	30.8	69.8	2.3	92
17	**1′b**	**3** (1 equiv,)	45	0.00	0	-	-	-	-	-
18	**1′b**	**3** (2 equivs.)	30	0.09	45	-	-	-	-	-
19	**1′b**	**3** (3 equivs.)	25	0.28	168	8.4	-	-	-	-
20	**1′b**	**3** (8 equivs.)	25	1.15	690	11	44.5	89.5	2.0	79
21	**1′b**	MMAO (30 equivs.)	20	0.00	0	-	-	-	-	-
22	**1′b**	MMAO (1000 equivs.)	20	1.68	1470	9.8	26.2	68.2	2.5	87
23	**2′a**	**3** (1 equiv.)	60	–	2.9[f]		-	-	-	-
24	**2′a**	**3** (3 equivs.)	60	0.50	25.0		-	-	-	-
25	**2′a**	**3** (5 equivs.)	60	0.85	42.5	∞	-	-	-	-
26	**2′a**	MMAO (1000 equivs.)	60	0.60	30.0	67	-	-	-	-
27	**2′b**	**3** (1 equiv.)	120	1.39	34.8		18.9	54.1	2.9	88
28	**2′b**	**3** (2 equivs.)	120	2.62	65,5		10.7	31.2	2.2	92
29	**2′b**	**3** (3 equivs.)	120	3.70	92,5	∞	14.7	61.1	4.2	88
30	**2′b**	**3** (10 equivs.)	120	4.59	114,8	489	14.4	40.5	2.8	91
31	**2′b**	MMAO (30 equivs.)	120	0.70	17.5		-	-	-	-
32	**2′b**	MMAO (1000 equivs.)	120	3.75	93.6	62	18.2	46.3	2.6	100

[a] *Experimental conditions:* solvent, toluene (50 mL), 30 °C, 5 bar, catalyst 4 μmol (Ni) or 20 μmol (Pd).
[b] Kg PE/mol·Ni·h.
[c] Catalyst half-life in min, calculated from ethylene consumption curves.
[d] M_n, $M_w \times 10^{-4}$.
[e] Number of Me branches/1000 C.
[f] Estimated from the ethylene consumption curve.

somewhat diminished by effect of the electron-withdrawing haloaryl groups.

Ethylene Polymerization Experiments

In order to evaluate the catalytic activity of the catecholate complexes **1′** and **2′**, we have performed a series of ethylene polymerization tests using MMAO, **3** or **4** as co-catalysts (Table 1). Treatment of the catecholate complexes with 1000 equivs. of MMAO leads to active polymerization catalysts. Compared to the corresponding nickel dihalide precursors **1a** and **1b**, the catecholate complexes **1′a** and **1′b** perform similarly (compare entries 4/12 and 16/22). The molecular weight and the branching contents of the polymers produced by catecholate and halide complexes are essentially the same indicating that both catalytic precursors lead to similar active species. Although we have not included the palladium halide complexes **2a** and **2b** in this study, the corresponding catecholate precursors **2′a** and **2′b** are also activated by MMAO (entries 26, 31 and 32). These results demonstrate the ability of the catecholate dianion to migrate from the transition metal center to aluminum. The ethyl organoaluminum derivative **4** also activates the nickel catecholate complex **1′a**, although not as efficiently as **3** (Table 1, entries 9 and 10).

When the blue solutions of nickel catecholate complexes are exposed to the cocatalyst (MMAO, **3** or **4**) under an ethylene atmosphere, a dramatic color change to magenta is observed, and ethylene polymer-

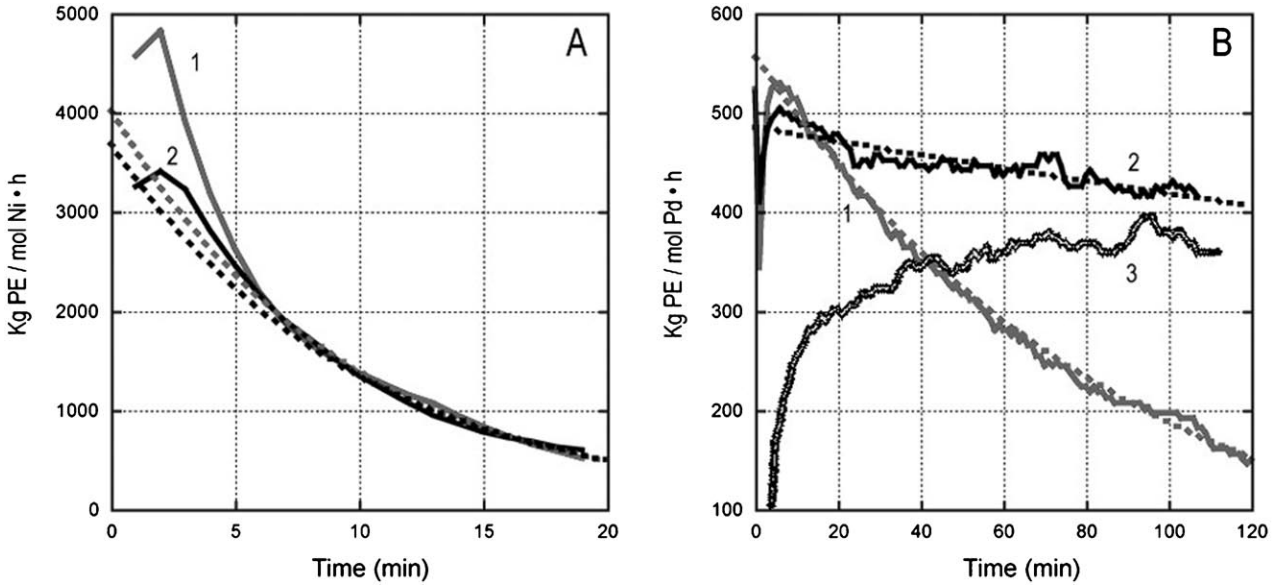

Figure 6. Catalytic activity curves for complexes **1′a** (**A**) and **2′b** (**B**) (solid lines) and first order curve fits (dashed lines). 1:MMAO, Al/M = 1000; 2:**3**M = 10:1; 3:**3**M = 3:1.

ization begins. Ethylene uptake curves confirm that the monomer consumption starts immediately, showing that the activation process is rapid. In those experiments where the ethylene consumption rate is high enough, the monomer uptake data can be accurately translated into instantaneous catalytic activity curves (Figure 6). These display a characteristic exponential decay profile, due to uniform catalyst deactivation. After the strong heat production in the initial minutes of the reaction, the system approaches thermal equilibrium and the activity curves can be fitted to first-order kinetic functions, allowing estimation of the catalyst half-life, which are collected in Table 3. Thus, although under our particular experimental conditions the Ni complexes **1b** and **1′b** display lower catalytic activity than **1a** and **1′a**, the former display significantly longer lifetimes, very likely as a consequence of the improved steric protection provided by the bulky *i*-Pr-substituted ligand. Interestingly, using MMAO in large excess does not improve the stability of the catalytic system as compared to co-catalyst **3** at much lower Al/M ratio, probably because the impurity scavenging effect of the alumoxane is not critical for Ni catalysts, which are known to be relatively tolerant to polar substances.

The aluminum compound **3** also activates the palladium catecholate complexes **2′a** and **2′b**, the latter being significantly more active. Ethylene consumption monitoring shows a milder reaction start than for the nickel complexes, attaining an activity maximum after several minutes, even when relatively large Al/Pd ratios are used (Figure 6 B). Low loadings of **3** can be equally efficient, but the activation process is slower, as noticed by the gradual increase of the ethylene uptake rate along the experiment (see curve 3 in Figure 6 B). Although much less active than their nickel analogues, the palladium catalysts **2′a** and **2′b** display longer lifetimes. Apparently, the stability of the Pd system is favored by low co-catalyst loading, and thus the use of **3** provides very long-lived catalysts. In contrast, activation with MMAO leads to relatively rapid catalyst deactivation, which explains the lower overall productivities obtained with this co-catalyst.

As already discussed, the activation of the Ni and Pd catecholate complexes requires comparatively low loads of **3**, and even equimolar amount of this cocatalyst can induce observable polymerization activities. The productivity of **1′a, 2′a** and **2′b** increases with the Al/M ratio, but beyond Al/M = 9 (molar ratio 3:1), this increase is less pronounced. The nickel derivative **1′b** behaves somewhat differently and its catalytic activity increases almost linearly with the Al/Ni ratio. Compared to MMAO, complex **3** appears to be a very efficient co-catalyst for the catecholate complexes. Even at the higher Al/M ratio explored for **3** (30:1), MMAO is still inactive. Interestingly, compound **3** becomes a much less efficient initiator with the halide precursors **1a** or **1b** suggesting that there is a positive cooperative effect in the catecholate-containing pre-catalyst/co-catalyst pair. This is highlighted in Figure 7, where the effect of MMAO and **3** on **1a** and **1′a** is compared. This observation suggests that, in accordance to our expectations, the catecholate exchange leads to the formation of some catecholaluminate counter-anion that is characterized by a low coordinating capability. Unfortunately, NMR techniques have not allowed us to detect this anionic species *in situ*, and attempts to isolate stable compounds from the catalytic system have hitherto been unsuccessful.

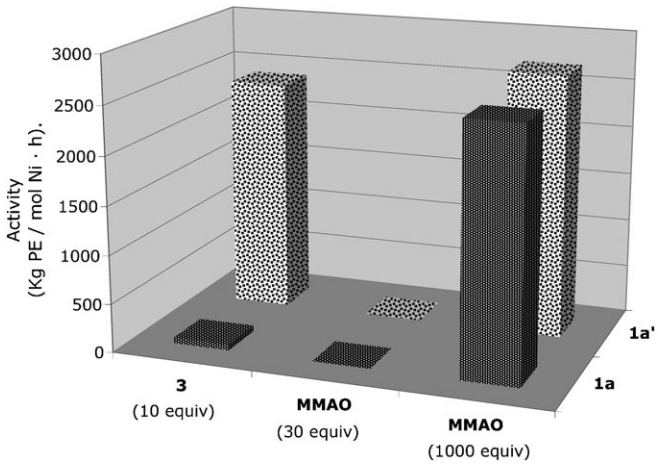

Figure 7. Comparative catalytic activities of the nickel catecholate **1′a** and halide **1a** complexes upon activation with compound **3** and MMAO.

Although a number of anionic alkoxoaluminates Al(O–O)$_2^-$ containing biphenols[24] or chelating siloxides[25] have been structurally characterized, to our knowledge catecholaluminate anions of the type Al(catecholate)$_2^-$, containing tetracoordinated aluminum have not been reported.

Besides the effect on reaction rates, the co-catalyst concentration has a significant influence on the structure of polyethylenes produced by the nickel complex **1′a**. As can be noticed (Table 3, entries 5–9), a consistent increase of the number of branches is observed as the **3**/**1′a** ratio varies from 1 to 10. In a parallel fashion, a moderate decrease (up to 50%) of M_n is observed, while the polydispersity index remains approximately constant. The same effect seems to operate with co-catalyst **4**, although the data available are very limited (entries 9 and 10). In comparison, polymers obtained with either **1a** or **1′a** and MMAO invariably display M_n values in the lower end of the range and high branching contents. This result is in line with the former trends, as MMAO is used in high Al/M ratio. However, these effects seem to be absent in the remaining catalysts.

Although many aspects of the ethylene polymerization with Ni and Pd α-diimine catalysts have been studied thoroughly,[26] the effect of the pre-catalyst/co-catalyst ratio has not received the same attention. Most studies implicitly assume that a large amount of alumoxanes (*ca.* 1:1000) is required in order to achieve optimum activities.[27] The influence of the Al/M ratio on the polymer structure has passed mostly unnoticed, but effects on the molecular weight and branching degree similar to those observed for **1a** and **1′a** have been briefly mentioned.[28] The decrease of the polymer molecular weight could be explained as a result of chain transfer to the co-catalyst, as has been observed in the iron-2,6-bisiminopyridine system.[29] The increase of the branching degree is more difficult to explain. However, considering that aluminum alkyl compounds have some capability to interact with the transition metal center through coordination, it is evident that these may have some influence on the polymer structure, which would increase with the concentration of cocatalyst. The coordination of co-catalyst at monomer binding site may render a species unable to insert new monomer units, without disrupting chain-walking or chain transfer processes, increasing the number of branches and decreasing molecular weight. These effects would be more noticeable for the more lewis-acidic Ni center than for Pd compounds and, obviously, should be favored by a lesser steric hindrance at the transition metal center. These conditions could favor the observation of the co-catalyst effect in the case of **1a** and **1′a**.

Conclusions

We have shown that, by means of an appropriate design of catalyst and co-catalyst components, a simple activation method for late transition metal ethylene polymerization system can be attained which avoids the use of large amounts of alumoxanes. Specifically, treatment of nickel and palladium α-diimine catecholate complexes (**1′**, **2′**) with alkylaluminum catecholates (**3, 4**) lead to active catalytic systems. The comparison of the catalytic activities achieved with combinations of α-diiminethe catecholate or halide complexes with different activators (MMAO, **3**, **4**) indicates that the presence of the catecholate ligand in both components of the catalyst favors high activity levels at very low M/Al ratio. The low M/Al ratio allowed by this catalytic activation protocol has some interesting advantages, such as increased catalyst stability, especially in the case of Pd. The positive effect of the catecholate ligand can be explained on the basis of two important considerations: i) The bidentate dianion is readily transferred from the late transition metal center to aluminum, in exchange for a monodentate alkyl group and ii) this exchange process takes place rapidly and irreversibly, affording a catalytically active ion pair formed by a coordinatively insaturated metal alkyl cation and a catecholaluminate anion. The low coordination capability of the latter appears to be an important feature to ensure a good catalytic activity. Further research is under way to ascertain the precise nature of the catalytic system generated by the catecholate-alkyl exchange process, and to find new pre-catalyst/co-catalyst combinations leading to improved catalytic activity. In addition, we are exploring the tolerance of these catalytic systems to polar substances and the possibility of polar monomer copolymerization.

Experimental Section

General Remarks

All manipulations were carried out under a dry nitrogen atmosphere by conventional Schlenk techniques. Solvents were rigorously dried by refluxing over sodium-benzophenone (toluene, hexane, diethyl ether, tetrahydrofuran) or calcium hydride (CH_2Cl_2) and freshly distilled prior to use. Deuterated solvents (Aldrich) were dried over CaH_2 (CD_2Cl_2, $CDCl_3$) or sodium-benzophenone (C_6D_6) and then distilled. $AlMe_3$ and $AlEt_3$ were purchased from Akzo-Nobel and used without further purification. Tetrachlorocatechol (Lancaster) was purified by filtration in toluene and then crystallized from CH_2Cl_2. Nickel and palladium dihalide complexes **1** and **2** were synthesized as reported in the literature.[21]

IR spectra were recorded from a Brucker Vector 22, and UV-VIS on a Perkin–Elmer model Lambda-12. NMR spectra were obtained on Bruker Avance DRX 400 (400 MHz) and Brucker Avance 300 (300 MHz) spectrometers. The ^1H and $^{13}C\{^1H\}$ resonances of the solvent were used as internal standard, but the chemical shifts (ppm) are reported with respect to TMS. Elemental analyses were performed by the Microanalytical Service of the Instituto de Investigaciones Químicas. Molecular weights of the polymers were determined by gel permeation chromatography employing universal calibration in a Waters 150c instrument with differential refractive index (DRI) detector and a Viscotek 150R DV detector.

Tetrachlorocatecholate Complexes 1′ and 2′

These compounds were prepared analogously: 450 mg (4 mmol) of solid potassium *tert*-butoxide were poured over a solution of tetrachlorocatechol (490 mg, 2 mmol) in 40 mL of THF at room temperature. The resulting solution of potassium tetrachlorocatecholate was dropwise added to a stirred solution or suspension of the appropriate dihalo α-diimine derivative **1** or **2** (2 mmol) in THF (20 mL) at room temperature. The stirring was continued for 4 h. The solution was filtered, and the solvent removed under reduced pressure. The residue was washed with 2×10 mL of hexane, and recrystallized from a mixture of CH_2Cl_2-hexane, to afford the product as dark blue crystals.

1′a: Yield: 0.95 g (80%). ^1H NMR (298 K, 300 MHz, CD_2Cl_2): δ = 7.28 (t, 2H, H *p*-CH_{ar}, $^3J_{H,H}$ = 5.1 Hz), 7.20 (d, 4H, H *m*-CH_{ar}, $^3J_{H,H}$ = 5.1 Hz), 2.49 (s, 12H, CH_3-Ar), 1.85 (s, 6H, CH_3-CN); $^{13}C\{^1H\}$ NMR (298 K, 75 MHz, CD_2Cl_2): δ = 172.1 (2C, C=N), 157.5 (2C, C_{cat}-O), 142.8 (2C, C_{ar}-N), 130.5 (4C, *o*-C_{ar}), 128.5 (2C, *p*-CH_{ar}); 128.2 (4C, *m*-CH, *m*-CH_{ar}), 116.7 (2C, C_{cat}-Cl), 115.1 (2C, C_{cat}-Cl), 18.6 (2CH_3-CN), 18.6 (4C, CH_3-Ar); IR (Nujol mull): ν = 806, 828, 981, 1227, 1291, 1531, 2361 cm^{-1}; UV (CH_2Cl_2, 10^{-4}M): λ (ε = 10^{-4} L mol^{-1} cm^{-1}) = 665 (0.67), 408 (0.56), 312 nm (1.60); MS (FAB): *m*/*z* = 616.980 [M+Na], calcd. for $C_{26}H_{24}N_2Cl_4O_2Ni$·Na: 616.984: anal. calcd. for $C_{26}H_{24}N_2Cl_4O_2Ni$·0.5 CH_2Cl_2: C 49.77, H 3.94, N 4.41; found: C 49.51, H 3.99, N 4.41.

1′b: Yield: 1.07 g (76%). ^1H NMR (298 K, 300 MHz, CD_2Cl_2): δ = 7.44 (t, 2H, *m*-CH_{ar}, $^3J_{H,H}$ = 7.5 Hz), 7.29 (d, 4H, *p*-CH_{ar}, $^3J_{H,H}$ = 7.5 Hz), 3.37 (h, 4H, $CHMe_2$, $^3J_{H,H}$ = 6.6 Hz), 1.85 (s, 6H, CH_3-CN), 1,53 (d, 12H, CHMeMe, $^3J_{H,H}$ = 6.45 Hz), 1.28 (d, 12H, CHMeMe, $^3J_{H,H}$ = 6.45 Hz); $^{13}C\{^1H\}$ NMR (298 K, 75 MHz, CD_2Cl_2): δ = 172.0 (2C, C=N), 157.7 (2C, C_{cat}-O), 140.9 (4*o*-C_{ar}), 140.0 (2C, C_{ar}-N), 128,8 (2C, *p*-CH_{ar}), 123.8 (4C, *m*-CH_{ar}), 116.4 (2C, C_{cat}-Cl), 114.9 (2C, C_{cat}-Cl), 30.0 (4C, $CHMe_2$), 24.1 (4C, CHMeMe), 23.5 (4C, CHMeMe), 19.2 (2C, CH_3-CN); IR (Nujol mull): ν = 807, 980, 1223, 1290, 1526, 1613 cm^{-1}; UV (CH_2Cl_2, 10^{-4}M): λ (ε = 10^{-4} L mol^{-1} cm^{-1}) = 690 (1.2), 395 (0.8), 315 nm (3.0); anal. calcd. for $C_{34}H_{40}Cl_4N_2NiO_2$·3 CH_2Cl_2: C 46.10, H 4.35, N 2.70; found, C 46.1, H 5.68, N 2.91.

2′a: Yield: 0.55 g (85%). ^1H NMR: (298 K, 300 MHz, CD_2Cl_2): δ = 7.30 (m, 6H, CH_{ar}), 2.39 (s, 12H, CH_3-Ar), 2.08 (s, 6H, CH_3-CN); $^{13}C\{^1H\}$ NMR: (298 K, 75 MHz, CD_2Cl_2): δ = 175.6 (2C, C=N), 159.0 (2C, C_{cat}-O), 142.7 (2C, C_{ar}-N), 129.8 (4C, *o*-C_{ar}), 128.9 (2C, *p*-CH_{ar}), 128.7 (4C, *m*-CH_{ar}), 116.87 (2C, C_{cat}-Cl), 115.6 (2C, C_{cat}-Cl), 18.8 (2C, C-CN), 18.4 (4C, Me-Ar); IR (Nujol mull): ν = 1435, 1264, 972 cm^{-1}; UV (CH_2Cl_2, 10^{-4}M): λ (ε = 10^{-4} L mol^{-1} cm^{-1}) = 660 (0.28), 380 (0.25), 307 (0.84), 250 nm (1.9); anal. calcd. C 48.44, H 3.75, N 4.35; found: C 48.33, H 4.30, N 4.74.

2′b: Yield: 0.65 g (80%). ^1H NMR (298 K, 300 MHz, CD_2Cl_2): δ = 7.44 (t, *p*-CH_{ar}, 2H, $^3J_{H,H}$ = 7.8 Hz), 7.33 (d, *m*-CH_{ar}, 4H, $^3J_{H,H}$ = 7.8 Hz), 3.11 (h, $CHMe_2$, 4H, $^3J_{H,H}$ = 6.75 Hz), 2.08 (s, Me-CN, 6H), 1.45 (d, CHMeMe 12H, $^3J_{H,H}$ = 6.75 Hz), 1.27 (d, CHMeMe, 12H, $^3J_{H,H}$ = 6.75 Hz); $^{13}C\{^1H\}$ NMR (298 K, 75 MHz, CD_2Cl_2): δ = 174.3 (2C, C=N), 159.0 (2C, C_{cat}-O), 140.0 (4C, *o*-C_{ar}), 139.9 (2C, C_{ar}-N), 129.3 (2C, *p*-CH_{ar}), 124.1 (4C, *m*-CH_{ar}), 117.0 (2C, C_{cat}-Cl), 115.9 (2C, C_{cat}-Cl), 29.6 (2C, $CHMe_2$), 24.19 (4C, CHMeMe), 23.87 (4C, CHMeMe), 19.3 (2C, CH_3-CN); IR (Nujol mull): ν = 1699, 1652, 1558, 1540, 1325, 803, 739 cm^{-1}; UV (CH_2Cl_2, 10^{-4}M): λ (ε = 10^{-4} L mol^{-1} cm^{-1}) = 710 (0.26), 390 (0.16), 312 (0.75), 251.13 nm (1.94); MS (FAB): *m*/*z* = 754.087 [M^+], calcd. for $C_{34}H_{40}Cl_4N_2O_2Pd^+$: 754.091; anal. calcd. for $C_{34}H_{40}Cl_4N_2O_2Pd$·0.33 C_6H_{14}: C 55.04, H 5.73, N 3.57; found: C 54.93, H 5.66, N 3.60.

Synthesis of Alkylaluminum Catecholates 3 and 4

A solution of tetrachlorocatecol (7.2 mmol) in CH_2Cl_2 (20 mL) was added dropwise to a cold (−80 °C) solution of "AlR_3" (10.8 mmol, R = Me, Et) in CH_2Cl_2 (20 mL). Stirring was continued for 30 min at the same temperature, and then 1 h at room temperature. The product crystallizes out when the colorless solution was stored at −30 °C overnight. Concentration and cooling provided successive crops.

3: Yield: 1.8 g (79%). ^1H NMR (298 K, 400 MHz, CD_2Cl_2): δ = −0.20 (s, 6H, Me-AlMe, terminal), −0.47 (s, 3H, Me-Al, central), −0.92 (s, 6H, Me-AlMe, terminal); $^{13}C\{^1H\}$ NMR (298 K, 75 MHz, CD_2Cl_2): δ = 142.0 (4 C, C_{cat}-O), 126.4 (4C, C_{cat}-Cl), 120.4 (4C, C_{cat}-Cl), −10.2 (4C, Me-AlMe, terminal), −12.4 (1C, Me-Al, central); IR, (KBr): ν = 2942, 2894, 1579, 1206, 1096, 1012, 977 cm^{-1}; anal. calcd. for $C_{17}H_{15}Al_3Cl_8O_4$: C 31.52, H 2.33, found: 31.30, H 2.11.

4: Yield: 1.55 g (60%). ^1H NMR (298 K, 300 MHz, CD_2Cl_2): δ = 1.25 (t, 6H, CH_3CH_2AlEt, terminal), 0.95 (t, 3H, CH_3CH_2Al, central), 0.67 (t, 6H,CH_3CH_2AlEt, terminal), 0.45 (q, 4H, CH_3CH_2AlEt, terminal), 0.20 (q, 4H, CH_3CH_2AlEt, terminal), −0.25 (q, 2H, CH_3CH_2Al, central); $^{13}C\{^1H\}$ NMR (298 K, 75 MHz, CD_2Cl_2): δ = 142.3 (4C, C_{cat}-O), 126.7 (4C, C_{cat}-Cl), 120.3 (4C, C_{cat}-Cl), 7.7 (1C, CH_3CH_2Al, central), 8.0 (2C, CH_3CH_2AlEt, terminal), 8.67

(2C, CH_3CH_2AlEt, terminal), −0.13 (1C, CH_3CH_2Al, central), −1.13 (1C, CH_3CH_2AlEt, terminal), −3.72 (1C, CH_3CH_2AlEt, terminal).

X-Ray Crystal Structure Analyses of 1′a, 1′b, 2′b and 3

A single crystal of each representative compound, of suitable size was mounted on a glass fiber using perfluoropolyether oil (FOMBLIN® 140/13, Aldrich) in the cold N_2 stream of the a low-temperature device attachment. A summary of crystallographic data and structure refinement is reported in the Supporting Information. Intensity data for complexes **1′a** to **3** were performed on a Bruker-AXS X8Kappa diffractometer equipped with an Apex-II CCD area detector, using a graphite monochromator Mo $K_{\alpha 1}$ ($\lambda =$ 0.71073 Å) and a Bruker Cryo-Flex low-temperature device. The data collection strategy used in all instance were phi and omega scans with narrow frames. Instrument and crystal stability were evaluated from the measurement of equivalent reflections at different measuring times and no decay was observed. The data were reduced (SAINT)[30] and corrected for Lorentz and polarization effects, and a semiempirical absorption correction was applied (SADABS)[31]. The structure was solved by direct methods (SIR-2002)[32] and refined against all F^2 data by full-matrix least-squares techniques (SHELXTL-6.14) minimizing $w[Fo^2-Fc^2]^2$. All the non-hydrogen atoms were refined with anisotropic displacement parameters. The hydrogen atoms were introduced into the geometrically calculated positions and refined riding on the corresponding parent atoms.

Crystallographic data (excluding structure factors) for the structures reported in this paper have been deposited with the Cambridge Crystallographic Data Centre as supplementary publication no. CCDC-643974 for **1′a**, CCDC-643975 for **1′b**, CCDC-6643976 for **2′b** and CCDC-6643977 for **3**. Copies of the data can be obtained free of charge on application to CCDC, 12 Union Road, Cambridge CB2 1EZ, UK [Facsimile: (+44)-01223-336033; e-mail: mailto:deposit@ccdc.cam.ac.uk], or *via* http://www.ccdc.cam.ac.uk/products/csd/request/

General Procedure for Ethylene Polymerization

A solution of the catalyst (4 μmol) in 50 mL of toluene was transferred under nitrogen atmosphere to a Fischer–Porter reactor equipped with a septum-capped port. The reactor was flushed three times with ethylene, and then allowed to equilibrate with this gas at the working conditions (5 bar/30 °C), using a thermostatted water bath. Then a solution of the co-catalyst, (either MMAO in heptane/toluene or aluminum complex **3** or **4** in toluene) was added with a syringe. Ethylene was feed from a small (150 mL) pressurized reservoir, using a regulator in order to maintain a constant reactor pressure. Ethylene consumption was continuously monitored by measuring the pressure drop at the reservoir. At the specified reaction time, the gas inlet was closed, the reactor vented and the reaction mixture poured over *ca.* 500 mL of methanol acidified with HCl, in order to precipitate the polymer. The mixture was stirred for 6 h, and the polymer precipitate separated by filtration and dried under vacuum until constant weight.

Supporting Information

Tables of selected bond distances and angles, crystal structure and refinement data for complexes **1′a, 1′b**, **2′a** and **3.**

Acknowledgements

Financial support from the DGI (Project CTQ2006–05527/BQU), Junta de Andalucía and Repsol-YPF is gratefully acknowledged. M. D. and E. T. gratefully thank research contracts from the European Union (Research and Training Network RTN1–1999–00164 "Polycat").

References

[1] a) H. Sinn, W. Kaminsky, H. J. Vollmer, R. Woldt, *Angew. Chem. Int. Ed. Engl.* **1980**, *19*, 390; b) H. Sinn, W. Kaminsky, *Adv. Organomet. Chem.***1980**, *18*.
[2] J. Scheirs, W. Kaminsky, *Metallocene-Based Polyolefins, Preparation, Properties and Technology*, Vol. 1., J. Wiley & Sons, Chichester, **2000**.
[3] V. C. Gibson, S. K. Spitzmesser, *Chem. Rev.* **2003**, *103*, 283.
[4] E. Y.-X. Chen, T. J. Marks, *Chem. Rev.* **2000**, *100*, 1391.
[5] a) M. Bochmann, *J. Organomet. Chem*, **2004**, *689*, 3982; b) I. Krossing, I. Raabe. *Angew. Chem. Int. Ed.* **2004**, *43*, 2066.
[6] M. D. Leatherman, S. A. Svejda, L. K. Johnson, M. Brookhart, *J. Am. Chem. Soc.* **2003**, *125*, 3068, and references cited therein.
[7] a) R. Fulton, A. W. Holland, D. J. Fox, R. G. Bergman, *Acc. Chem. Res.* **2002**, *35*, 44; b) H. E. Bryndza, W. Tam, *Chem. Rev.* **1988**, *88*, 1163.
[8] F. A. Cotton, G. Wilkinson, C. A. Murillo, M. Bochmann, *Advanced Inorganic Chemistry*, 6th edn., J. Wiley & Sons, New York, **1999**, p 187.
[9] M. V. Metz, Y. Sun, C. L. Stern, T. J. Marks, *Organometallics* **2002**, *21*, 3691.
[10] C. Makedonas, C. A. Mitsopoulou, F. J. Lahoz, and A. I. Balana. *Inorg. Chem.* **2003**, *42*, 8853.
[11] T. B. Karpishin, M. S. Gebhard, E. I. Solomon, K. N. Raymond, *J. Am. Chem. Soc.* **1991**, *113*, 2977–2984.
[12] D. J. Tempel, L. K. Johnson, P. L. Huff, P. S. White, M. Brookhart, *J. Am. Chem. Soc.* **2000**, *122*, 6686.
[13] E. K. Cope-Eathough, F. S. Mair, R. G. Pritchard, J. E. Warren, R. J. Woods, *Polyhedron* **2003**, *22*, 1447.
[14] J. Feldman, S. J. McLain, A. Parthasaraty, W. J. Marshall, J. C. Calabrese, S. D. Arthur, *Organometallics* **1997**, *16*, 1514.
[15] a) C. G. Pierpont, T. M. Buchanan, *Coord. Chem. Rev.* **1981**, *38,* 45; b) W. P. Griffith, *Transition Met. Chem.* **1993**, *18*, 250; c) C. G. Pierpont, C. W. Lange, *Prog. Inorg. Chem.* **1994**, *41*, 331; d) C. G. Pierpont, *Coord. Chem. Rev.* **2001**, 415, 219–221; e) D. N. Hendrickson, C. G. Pierpont, *Topics Curr. Chem.* **2004**, *234,* 63–95; f) P. Zanello, M. Corsini. *Coord. Chem. Rev.* **2006**, *250*, 2000.
[16] C. G. Pierpont. *Coord. Chem. Rev.* **2001**, *216*, 99.

[17] a) C. Bruckner, D. L. Caulder, K. N. Raymond, *Inorg. Chem.* **1998**, *37*, 6759; b) G. A. Fox and C. G. Pierpont. *Inorg. Chem.* **1992**, *31*, 3718; c) C. W. Lange, C. G. Pierpont, *Inorg. Chim. Acta* **1997**, *263*, 219; d) D. Herebian, E. Bothe, F. Neese, T. Weyhermuller, K. Wieghardt, *J. Am. Chem. Soc.* **2003**, *125*, 9116.
[18] a) H. F. Klein, E. Auer, A. Dal, U. Lemke, T. Jung, C. Rohr, U. Florke, H. J. Haupt, *Inorg. Chim. Acta* **1999**, *287*, 167; b) N. Okabe, Y. Muranishi, T. Aziyama, *Acta Crystallogr. Section E: Online Reports*, **2003**, *59*, M936.
[19] a) H. Ohtsu, K. Tanaka, *Angew. Chem. Int. Ed.* **2004**, *43*, 6301; b) M. W. Lycnch, R. M. Buchanan, C. G. Pierpont, D. N. Hendrickson, *Inorg. Chem.* **1981**, *20*, 1038.
[20] a) O. Carugo, C. B. Castellani, K. Djinóvic, M. Rizzi, *J. Chem. Soc., Dalton Trans.* **1992**, 837; b) O. Carugo, K. Djinóvic, M. Rizzi, C. B. Castellani, *J. Chem. Soc., Dalton Trans.* **1991**, 1551.
[21] W. Ziemkowska, *Main Group Metal Chemistry,* **2000**, *23*, 337.
[22] See, for example: a) J. Lewinski, J. Zachara, *J. Organomet. Chem.* **1998**, *560,* 89; b) W. Ziemkowska, S. Pasynkiewicz, T. Glowiak, *J. Organomet. Chem.* **1998**, *562*, 3; c) C. N. McMahon, S. J. Obrey, A. Keys, S. G. Bott, A. R. Barron, *J. Chem. Soc., Dalton Trans.* **2000**, 2151; d) W. Ziemkowska, *Polyhedron* **2002**, *21*, 281; e) C. N. McMahon, L. Alemany, R. L. Callender, S. G. Bott, A. R. Barron, *Chem. Mater.* **1999**, *11*, 3181; f) W. Uhl, R. Gerding, A. Vester, *J. Organomet. Chem.* **1996**, *513*, 163.
[23] CCDC database 5.28 (November, 2006), average over 12 related structures including **3**.
[24] a) H. Nöth, A. Schlegel, M. Suter, *J. Organomet. Chem*, **2001**, *621*, 231; b) T. Arai, H. Sasai, K. Aoe, K. Okamura, T. Date, M. Shibasaki, *Angew. Chem. Int. Ed.* **1996**, *35*, 104.
[25] Y. K. Gun′ko, R. Reilly, V. G. Kessler, *New J. Chem.* **2001**, *4*, 528.
[26] D. P. Gates, S. A. Svejda, E. Oñate, C. M. Killian, L. K. Johnson, P. S. White, M. Brookhart, *Macromolecules* **2000**, *33*, 2320.
[27] L. K. Johnson, C. M. Killian, M. Brookhart, *J. Am. Chem. Soc.* **1995**, *117*, 6414.
[28] a) F. Zhu, W. Xu, X. Liu, S. Lin, *J. Appl. Polym. Sci.*, **2001**, *84*, 1123; b) K. R. Kumar, S. Sivaram, *Macromol. Chem. and Phys.*, **2000**, *201*, 1513.
[29] a) B. L. Small, M. Brookhart, *Macromolecules* **1999**, *32*, 2120; b) G. J. P. Britovsek, M. Bruce, V. C. Gibson, B. S. Kimberley, P. J. Maddox, S. Mastroianni, S. J. McTavish, C. Redshaw, G. A. Solan, S. Strömberg, A. J. P. White, D. J. Williams, *J. Am. Chem. Soc.* **1999**, *121*, 8728.
[30] SAINT+, Bruker-APEX 2 package. Version 2.1. Bruker Analytical X-ray Solutions, Madison, Wisconsin, USA, **2006**
[31] SADABS, Bruker-APEX 2 package. Version 2.1. Bruker Analytical X-ray Solutions, Madison, Wisconsin, USA, **2006**.
[32] M. C. Burla, M. Camalli, B. Carrozzini, G. L. Cascarano, C. Giacovazzo, G. Polidori, R. Spagna, SIR2002: the program; *J. Appl. Cryst*, **2003**. *36*, 1103; SHELXTL 6.14, Bruker AXS, Inc., Madison, Wisconsin, USA, **2000–2003**.

